Constraints on surface NO_x emissions by assimilating satellite observations of multiple species

Kazuyuki Miyazaki[1] and Henk Eskes[2]

Received 9 July 2013; revised 12 August 2013; accepted 21 August 2013; published 6 September 2013.

[1] Surface NO_x emissions are estimated by a combined assimilation of satellite observations of NO_2, CO, O_3, and HNO_3 with a global chemical transport model. The assimilation of measurements for species other than NO_2 provides additional constraints on the NO_x emissions by adjusting the concentrations of the species affecting the NO_x chemistry and leads to changes in the regional monthly-mean emissions of −58 to +32% and the annual total emissions of −16 to +3%. These large changes highlight that uncertainties in the model chemistry impact the quality of the emission estimates. In the inversion from NO_2 observations only, NO_x analysis increments occur closer to the surface. Because of the shorter residence time, larger emissions increments are required compared to the multiple species assimilation. Validation against independent observations and comparisons with the recent Regional Emission inventory in Asia version 2.1 emissions shows that the multiple species assimilation improves the chemical consistency including the relation between concentrations and the estimated emissions. **Citation:** Miyazaki, K., and H. Eskes (2013), Constraints on surface NO_x emissions by assimilating satellite observations of multiple species, *Geophys. Res. Lett.*, *40*, 4745–4750, doi:10.1002/grl.50894.

1. Introduction

[2] Nitrogen oxides (NO_x) in the atmosphere have a large impact on air quality and climate. Among the many factors influencing tropospheric NO_x variations, surface emissions of NO_x play an important role but typically have large uncertainties [e.g., *Zhao et al*., 2011 and references therein]. NO_x emission estimates have been obtained by combining tropospheric NO_2 satellite retrievals with assimilation or inversion technique [e.g., *Martin et al*., 2003; *Jaeglé et al*., 2005; *Boersma et al*., 2008; *Zhao and Wang*, 2009; *Miyazaki et al*., 2012a]. These estimates rely on the relationship between the NO_2 concentration and NO_x emissions being realistically simulated by the model. However, there are many sources of error in current chemical transport models (CTMs), including chemical reaction rates, advection, convective transport, boundary layer mixing, deposition, and emissions of other precursors. These uncertainties impact the accuracy of the NO_x emission inversion [*Lin et al*., 2012; *Stavrakou et al*., 2013].

[3] As a result of recent developments in satellite instrumentation for detecting various chemical compounds in the troposphere, there is an increasing interest in combining observations of multiple species to improve the analysis of the tropospheric chemical system, including the emissions. Through their chemical interactions with NO_x, other species such as O_3 and HNO_3 influence the NO_x emission estimates. *Miyazaki et al*. (2012b, hereafter M2012b) demonstrated that the assimilation of observations of multiple species is a powerful approach to constrain the tropospheric chemical system by simultaneously adjusting the chemical concentrations and emission fields. Although M2012b showed that multiple species assimilation provides additional constraints on the emission inversion, its detailed impact and the seasonal dependence have not been addressed.

[4] In this study, we use the multivariate data assimilation system of M2012b to estimate the impact of non-NO_2 observations on the NO_x emission inversion through the improved estimates of atmospheric fields and emission fluxes affecting the NO_x chemistry. Global surface NO_x emissions and their seasonal variations in 2007 are estimated from a full year multispecies data assimilation run compared to an emission inversion run using NO_2 observations only.

2. Assimilated Satellite Data

[5] We assimilated the following satellite observations into the global CTM Chemical AGCM for Study of Atmospheric Environment and Radiative Forcing (CHASER) (M2012b): O_3 obtained from Tropospheric Emission Spectrometer (TES), CO from Measurement of Pollution in the Troposphere (MOPITT), NO_2 from Ozone Monitoring Instrument (OMI), and O_3 and HNO_3 from Microwave Limb Sounder (MLS). The OMI NO_2 data used were the DOMINO version-2 product. The high temporal and spatial resolutions (13 × 24 km at nadir) of the OMI tropospheric NO_2 column retrievals are useful for constraining daily global NO_x emissions. The TES O_3 data used are the version 4 level-2 nadir data obtained from the global survey mode. These data have a spatial resolution of 5–8 km and a vertical resolution of typically 6 km. The MOPITT CO data employed are the version 5 level 2 TIR data. We also used the version 3.3 level 2 MLS products for pressures lower than 215 hPa for O_3 and 150 hPa for HNO_3. The observational errors in each retrieval included smoothing error, systematic error, and measurement error. A more extended description of the observations including their references, data quality, and data filtering methods employed is given in M2012b.

[6] The observation operator, *H*, which consists of the spatial interpolation, S, the state conversion by the averaging

Additional supporting information may be found in the online version of this article.

[1]Japan Agency for Marine-Earth Science and Technology, Yokohama, Kanagawa, Japan.
[2]Royal Netherlands Meteorological Institute, De Bilt, Netherlands.

Corresponding author: K. Miyazaki, Japan Agency for Marine-Earth Science and Technology, 3173-25 Showa-machi, Kanazawa-ku, Yokohama, Kanagawa 236-0001, Japan. (kmiyazaki@jamstec.go.jp)

0094-8276/13/10.1002/grl.50894

kernel, A, and the a priori profile, x^a, was applied for each retrieval to convert the model fields, x, to the observation space, y^b, in the data assimilation,

$$y^b = H(x) = x^a + A(S(x) - x^a). \quad (1)$$

[7] The averaging kernel accounts for the vertical sensitivity and intrinsic vertical resolution of the satellite measurement. By using this operator, the relative satellite-model difference $(y^o - y^b)/y^o$ is not sensitive to the a priori profile x^a (Eskes and Boersma, 2003) for an optically thin absorber like NO_2.

3. Data Assimilation System

[8] The data assimilation system, CHASER-DAS, simultaneously optimizes the surface emissions of NO_x and CO, the lightning sources of NO_x, and the concentrations of all of the predicted chemical species (total 35) in all grid cells of the model for each data assimilation cycle (every 100 min). It is based on the CHASER CTM and an ensemble Kalman filter (EnKF) technique. CHASER-DAS allows us to fully exploit the detailed chemical and physical processes in the model through the use of ensemble simulations for estimating the background error covariance, as described in M2012b.

[9] Several modifications have been made to the configuration used in M2012b. First, the a priori NO_x emissions have been updated to newer inventories: Emission Database for Global Atmospheric Research version 4.2 (yearly anthropogenic emissions), Global Fire Emissions Database version 3.1 (monthly biomass burning emissions), and Global Emissions Inventory Activity (monthly soil emissions) for the analysis in 2007. In M2012b, older emissions inventories for 1995 and 2000 were extrapolated to the simulation years 2006–2007 assuming a constant trend, which resulted in spurious analysis increments regionally. Second, the calculation period is extended to the entire year 2007 with a longer spin-up calculation. We performed twelve 1 month calculations from the first day of each analysis month after a 15 day spin-up data assimilation calculation for each 1 month calculation. The initial conditions for the 15 day spin-up calculation were obtained from a 1 year CHASER simulation. Considering the short lifetime of tropospheric chemical species and the large amount of the observations used, the spin-up period is considered to be sufficiently long.

[10] We conducted several data assimilation runs: a multisatellite data sets assimilation (MDA) run, a single data set assimilation (SDA) run, and observing system experiments (OSEs). In the MDA run, all of the satellite data sets were assimilated to simultaneously optimize the emissions and concentrations. In the SDA run, only OMI NO_2 data were assimilated to optimize surface NO_x emissions only. In the OSEs, we removed one of the assimilated data sets to measure the impact of the individual observation types on the results of the emission analysis. In all cases, non-NO_2 observations influence NO_x emissions through adjustments of the concentration fields. In the EnKF data assimilation, a new analysis and its ensemble perturbation matrix are simultaneously obtained by transforming the background ensemble. The analysis ensemble spread obtained is used as measure of the a posteriori uncertainty of NO_x emissions.

[11] The overall performance of CHASER-DAS was evaluated based on comparisons against independent global ozonesonde, aircraft, and satellite observations in M2012b. The multispecies data assimilation significantly reduced both global mean bias (by up to 90%) and root-mean-square error (RMSE) (by up to 50%) of the monthly-mean concentrations against the assimilated and independent data sets for various chemical fields (e.g., NO_2, O_3, HNO_3, CO, and PAN), compared to the results obtained from assimilation of OMI NO_2 observations only, as shown in M2012b (e.g., Figure 5). The improvements include a reduced CO bias in the Northern Hemisphere (NH) lower troposphere (by 40–90%), a reduced negative HNO_3 bias in the extratropical upper troposphere (by up to 85%), and a reduced positive O_3 bias from the middle troposphere to the lower stratosphere (from 30–40% to within 10%). M2012b demonstrated that all the assimilated data sets contribute to reduce the O_3 bias in July 2007 by their influences on the precursor emissions and chemical processes that affect the O_3 concentration.

4. Estimated Surface NO_x Emissions

[12] Figure 1 shows the global map of the annual NO_x emissions obtained from the a priori inventories and the MDA run. The total annual global emissions in the MDA run were 44.5 TgN, which is about 12% higher than the a priori emissions. Large positive increments in the annual emissions were found over eastern China (37% in the regional annual total emissions, as defined in Figure 2), the eastern United States (15%), northern and central Africa (+45%), southern Africa (+67%), Southeast Asia (+17%), and Australia (113°E–155°E, 44°S–11°S, +39%), whereas the increments were negative over South America (−38%) and Canada (141°W–52°W, 41°N–70°N, −35%). The increases in the total annual global emissions can be primarily attributed to large positive increments in the NH during the early summer (May–July), as shown in Figure 2. The total hemispheric monthly analysis increment reached 38% in the NH in July and 46% in the Southern Hemisphere (SH) in October, respectively.

[13] The a priori emissions were created based on the emission inventories, in which the emissions from biomass burning and soil were reported on a monthly basis, whereas the seasonal variation of anthropogenic emissions was not considered in either the inventories or the CHASER simulation. As a result, the implemented a priori emissions show distinct seasonal variations only over the major biomass burning areas. Data assimilation introduces significant seasonal emission variations over most continents, and a large seasonality is observed over polluted regions (e.g., Europe, east Asia, India, and the United States). The timing of the peak emissions is also changed by the data assimilation; it is earlier by 1–2 months over North America, southern Europe, and southern parts of the Eurasian continent, typically from July to June. In contrast, the timing is delayed by a few months over India and some parts of central and southern Africa. The a posteriori emissions over Southeast Asia have two maxima in March and July. This distinct seasonal variation is not represented by either the emission inventories or the CHASER simulation. The results for the biomass regions indicate that the a priori annual NO_x emission from fires in South America is overestimated by 37%, and Central Africa is underestimated by 45% in 2007, possibly mainly because of large uncertainties in emission

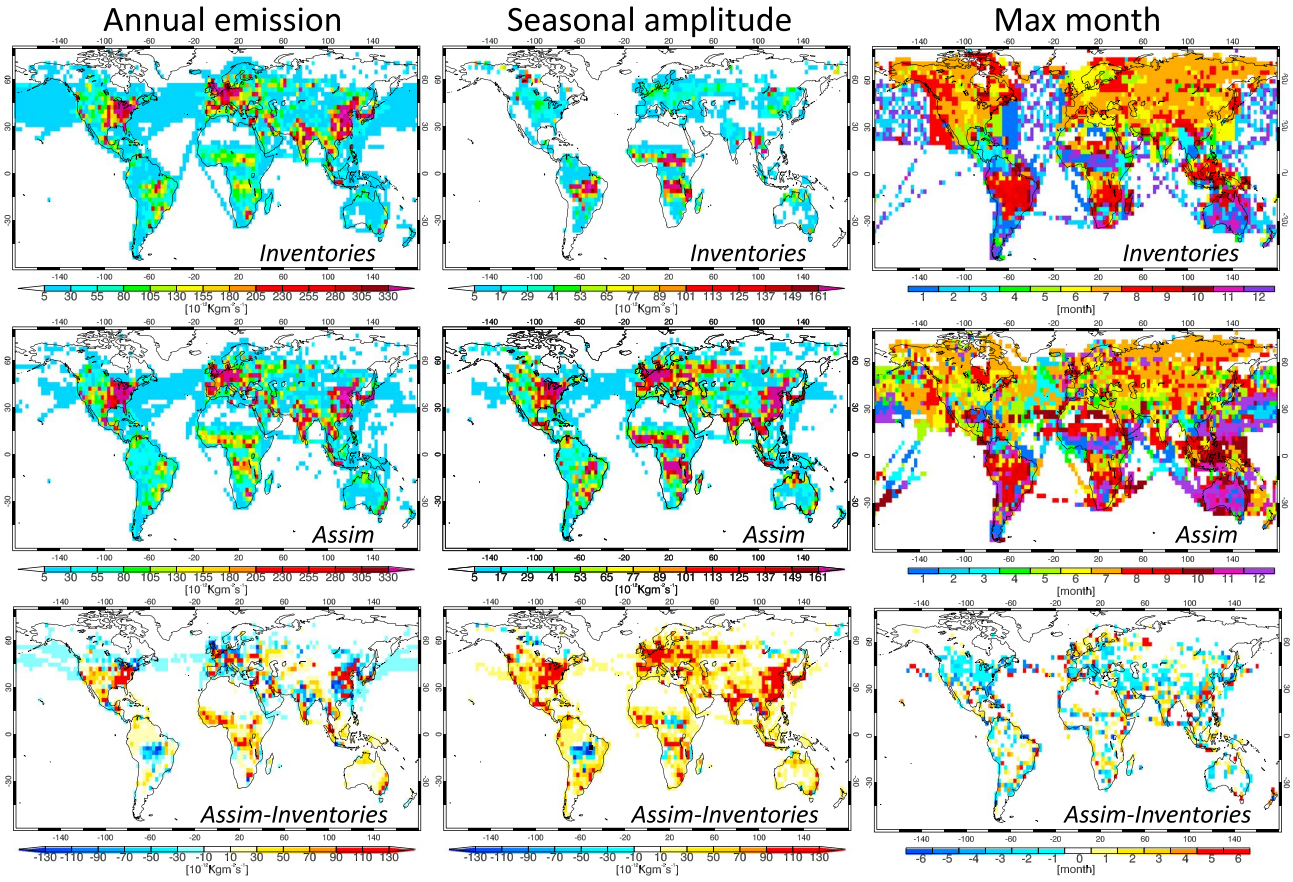

Figure 1. Global distributions of the (left column, in 10^{-12} kgm^{-2}s^{-1}) annual surface NO_x emissions, its (middle column, in 10^{-12} kgm^{-2}s^{-1}) seasonal amplitude, and the (right column, in month) timing of peak emissions in 2007. The (top row) a priori emissions, the (middle row) a posteriori emissions, and the (bottom row) analysis increment (a posteriori minus a priori emissions) are shown for each panel. For the analysis increment of the seasonal amplitude and the timing of peak emissions, the results are shown for the region with annual emissions of greater than 10^{-11} kgm^{-2}s^{-1}.

factors used in the inventories but the seasonality is described reasonably. The a posteriori uncertainty does not include the a priori emissions in most cases.

[14] Over eastern China, the a priori annual emissions were lower than the newer emission inventory, Regional Emission inventory in Asia version 2.1 (REAS 2.1) [*Kurokawa et al.*, 2013], by a factor of 0.65 (3.81 versus 5.87 TgN). Compared to the a priori emissions, the REAS inventory has employed more up to date data that reflect the Chinese emissions in 2007. Data assimilation changes the total annual emissions from 3.81 to 5.28 TgN, with large increases around large cities (Figure S1). The a posteriori emissions show a much improved agreement with the REAS 2.1 emissions in their magnitude, seasonal variation, and spatial distribution compared to the a priori emissions. The difference between the a posteriori and REAS emissions is generally within the range of the a posteriori uncertainty (±0.72 TgN in annual mean, as plotted in Figure 2).

[15] *Zhao and Wang* [2009] estimated the regional emission of 11.0 TgN over East Asia (80°E–150°E, 10°N–50°N) for July 2007 from OMI observations, which is close to our MDA estimate of 11.6 TgN. The 0.465 TgN estimated over the eastern United States (102°W–64°W, 22°N–50°N) from the OMI observations for March 2006 [*Boersma et al.*, 2008] is also close to our MDA estimate of 0.433 TgN but for March 2007. While our MDA estimates agree with these previous results, the small differences may be attributed to differences in the retrieval data, the forecast model, and the inversion approach including the use of non-NO_2 measurements. In both cases, the a priori emissions are lower (10.0 and 0.377 TgN) and the SDA emissions are higher (13.2 and 0.439 TgN) than the MDA emissions.

[16] The summertime peaks over the northern midlatitude regions are likely due to enhanced emissions by soils. *Jaeglé et al.* [2005] and *Wang et al.* [2007] suggested that soil emissions at northern midlatitude regions including Europe, the United States, and East Asia account for nearly half of the fuel combustion sources during summer. In addition, they estimated that the a priori inventories largely underestimate the soil sources with a factor of 2–3. Our estimates consistently show large increases in the summertime sources at the northern midlatitudes, where the regional difference in the seasonality can be attributed to differences in the timing of fertilizer application and the influence of seasonally variable environmental factors including temperature and precipitation, as suggested by *Wang et al.* [2007].

5. Impact of Multispecies Data Assimilation

[17] The spatial pattern of the emission analysis increments from the MDA and SDA runs is generally similar. In contrast, the absolute magnitude of the analysis increments

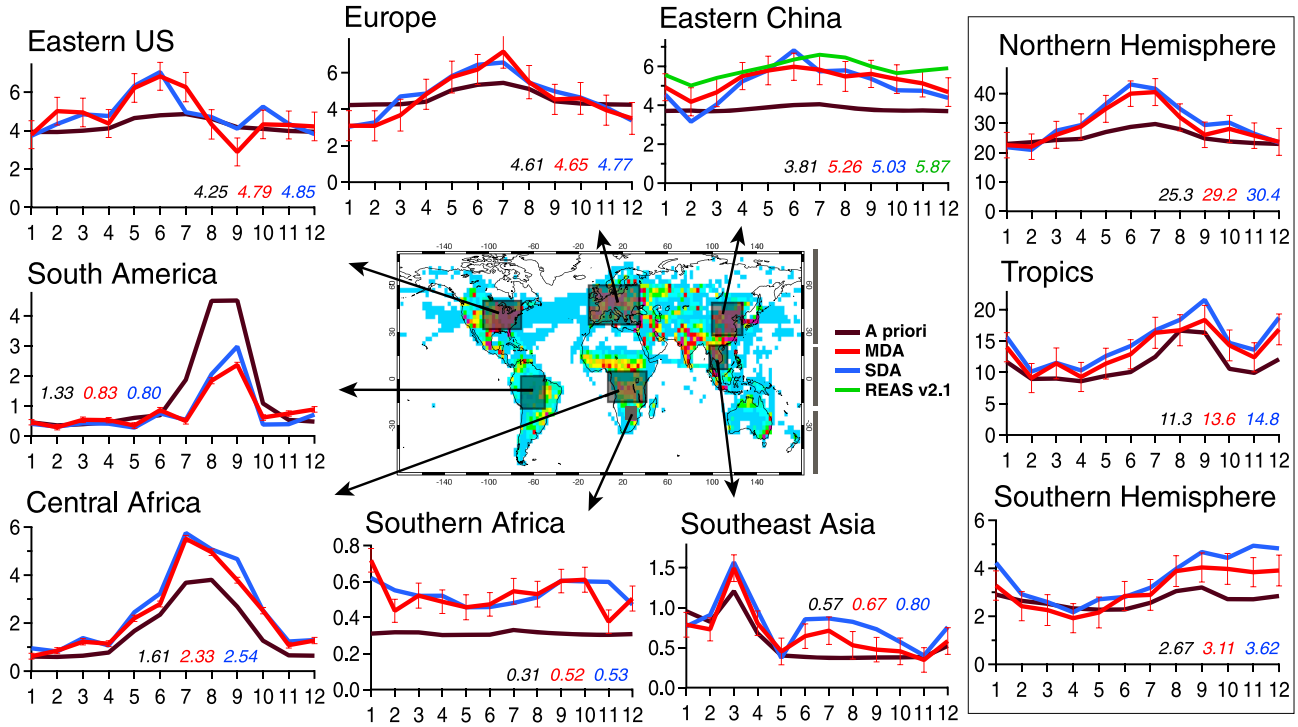

Figure 2. Seasonal variations of the regional surface NO_x emissions (in TgN) for the northern hemisphere (20°N–90°N), the Tropics (20°S–20°N), the Southern Hemisphere (90°S–20°S), eastern China (105°E–123°E, 25°N–40°N), Europe (10°W–30°E, 35°N–60°N), the eastern United States (102°W–70°W, 28°N–50°N), South America (70°W–50°W, 20°S–Equator), central Africa (10°E–40°E, 20°S–Equator), southern Africa (26°E–31°E, 28°S–23°S), and Southeast Asia (96°E–105°E, 10°N–20°N) for 2007. The a priori emissions (black line), the a posteriori emissions obtained from the MDA (red line) and SDA (blue line) runs, and the REAS 2.1 data (green line) are plotted. The error bar for the MDA emission represents the a posteriori emission uncertainty estimated from the analysis ensemble spread. The total annual values (in TgN) for each emission are displayed in each panel.

differs significantly between the two runs in many regions, as a consequence of the NO_2 profiles being modified by the non-NO_2 observations. The difference (SDA minus MDA) in the monthly total emissions was −4 to +13% in the NH, +3 to +18% in the Tropics, and −1 to +29% in the SH, respectively. The total emissions are generally higher in the SDA run than in the MDA run (e.g., total annual global emissions are about 6% higher), suggesting that the SDA system overcorrects the emissions in many regions. On the regional scale, the differences are more obvious and complex; the monthly and annual total regional emission differences (SDA minus MDA) ranged from −32 to +58% and from −3 to +16%, respectively. The regional emission differences were tightly associated with changes in the relative ratio of the lower and upper tropospheric NO_2 abundance due to the assimilation of non-NO_2 measurements.

[18] Large (mostly positive) analysis increments in the NO_x concentration were found in the upper troposphere in the MDA run owing to the high sensitivity of TES to O_3 concentrations at these altitudes, and large abundance of MLS observations. In the SDA run, in contrast, only the surface emissions are optimized, and the concentration fields are thus modified primarily near the surface. Owing to the altitude dependence of the chemical lifetime of NO_x (i.e., longer at higher altitudes), the residence time of the NO_x increments can be significantly different between the two runs. In fact, the mean chemical loss rate of tropospheric NO_x was higher in the SDA run than in the MDA run, with a larger difference in July (14%) than in January (8%), reflecting larger NO_x amounts in the NH than in the SH and the faster photochemical processing. The mean HNO_3 production rate by the reaction of NO with HO_2 was larger in the SDA run than in the MDA run by 15% in July and by 3% in January, respectively, while those by the reaction of NO_2 with OH was stronger only in July by 4%. In the SDA run, NO_x analysis increments occur closer to the surface and are removed more quickly, and larger emission increments are required compared to the MDA run, especially in summer. Note that the detailed chemical response to the data assimilation process is more complex. For example, the oxidation rates of nonmethane volatile organic compounds, including isoprene, are also changed through data assimilation by up to +6% for the tropospheric mean, which will also influence the organic nitrate formation and the NO_x lifetime.

[19] The validation results of the concentrations simulated using the estimated emissions are summarized in Table S1. By using the SDA estimated NO_x emissions instead of the emission inventories, CHASER simulations showed improved agreement with independent global ozonesonde and satellite observations. The CHASER simulation showed further improved agreement by changing the emission data from the SDA emissions to the MDA emissions (the direct concentration adjustment by assimilation is not applied in these cases). The improved agreement includes large reductions in the ozone positive bias against ozonesonde observations in the middle (from +2.0 to +0.1 ppbv) and upper (from +2.5 to +0.3 ppbv) troposphere for the Tropics, and 20–50% reductions in the positive bias and slight increases in the

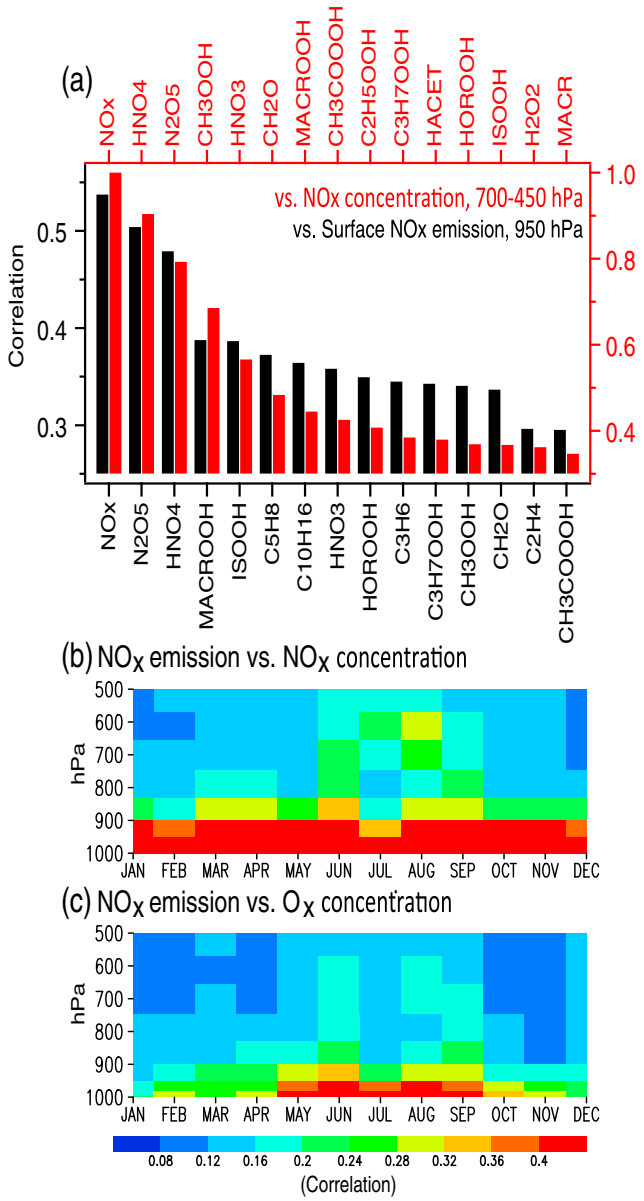

Figure 3. (a) Correlations between surface NO_x emissions and concentrations of chemically related species estimated from the background error covariance at 950 hPa (black) and the correlations between the NO_x concentration and the concentration of chemically related species averaged between 700 and 450 hPa (red) over eastern China averaged in the daytime over the year 2007. The 15 most correlated chemical species from the 35 forecasted species in CHASER are listed. (b) Time-height cross section of the correlation between surface NO_x emissions and the NO_x concentration (black), and (c) between surface NO_x emissions and the O_x concentration in 2007.

spatial correlation in monthly-mean tropospheric NO_2 columns against GOME-2 and SCIAMACHY measurements. Comparisons against the TES and MLS O_3 profile retrievals and the tropospheric ozone column retrievals also reveal improvements (i.e., 10–20% reductions in the global/monthly-mean bias and RMSE in most cases, except for the lower tropospheric bias) by using the MDA emissions throughout the troposphere. This demonstrates the improved consistency of the concentrations and emissions in the MDA analysis with all available observations, and indicates that the non-NO_2 measurements provide important information to improve the surface NO_x source estimates.

[20] The OSEs confirmed that the direct adjustment of the concentrations with the MLS and TES data has an important effect on the emission inversion. The relative importance of individual measurements differs greatly between regions, as summarized in Table S2. For instance, in July 2007, an emission increase of about 9% in the MDA run compared to the SDA run is primarily attributed to the assimilation of the TES data over Europe. The assimilation of MOPITT CO data generally decreases the free tropospheric OH concentration in the NH extratropics by 2–5% and increases the lifetime of NO_x corresponding to the increased surface CO emissions (from 1191 TgC (the a priori) to 1347 TgCO as the annual global total). The MOPITT CO impact on the regional NO_x emission estimate was typically less than 5% (mostly negative).

[21] Biases in any of the measurement data sets may seriously degrade the overall performance of the data assimilation. *Miyazaki et al.* [2012b] demonstrated that possible biases (up to 40%) in the NO_2 retrieval change regional NO_x emissions by 5–45% and seriously degrade the emission analysis. Systematic errors in the OMI NO_2 retrievals used in this study were estimated to be $-10 \pm 14\%$ over east Asia [*Irie et al.*, 2012], which may cause biases in the estimated emissions. The emission estimates may also be sensitive to measurement biases for species other than NO_2. We confirmed that a bias correction for the positive bias in the TES O_3 profiles (a uniform 3.3 (6.5) ppbv bias above (below) 500 hPa, as recommended by *Worden et al.*, 2009) decreased the regional monthly NO_x emissions by 1–11% and the global monthly total emissions by 1–2% in the MDA analysis.

[22] Although the tropospheric NO_2 column measurements generally do not contain information on the vertical profiles of NO_x sources, the use of the multiple data sets effectively constrained the vertical profiles of the sources throughout the troposphere, distinguishing between the surface and lightning in our MDA estimates. The inclusion of lightning changes the surface emissions by up to 12% over eastern China and 4% over the eastern United States in summer, as shown in Table S3. This finding demonstrates the importance of assimilating multiple satellite data sets for the analysis of surface NO_x emissions. In contrast, changing the relative magnitude for the a priori error for the surface and lightning sources by 20% leads to only minor changes to the analyzed surface emission (Table S3). These results demonstrate the robustness of the emissions estimated from the MDA run. Emission inversions for individual source categories may improve the understanding of the mechanisms responsible for the seasonal variations and are important topic for future studies.

6. Discussion and Conclusions

[23] The multispecies data assimilation puts additional constrains on the NO_x emissions through the improvement in atmospheric fields and emission fluxes influencing the NO_x chemistry. The emissions estimated from multiple species assimilation are generally closer to the a priori emissions than those estimated from NO_2 observations only. The large difference between the two estimates highlights that model errors in various species fields cause a large uncertainty in NO_x emissions when derived from NO_2 observations only.

[24] Model performance is critical for the correct propagation of observational information between chemical species and to improve the emission estimation. Model errors in, for instance, atmospheric transports and lightning NO_x sources could have large influences on the emission estimation, as discussed by *Miyazaki et al*. [2012b] and *Lin et al*. [2012]. The diurnal variability of the emissions will also influence the estimate; e.g., neglecting the variability changes regional monthly emissions by about 5–65% [*Miyazaki et al*., 2012b]. Owing to the common anthropogenic and biomass burning sources for various species, an appropriate consideration of the correlation between the multiple species emissions for the each source category might help to directly improve the NO_x emissions from various observations. Improvements in the model, data assimilation scheme, and retrieved observations are thus essential to reduce the uncertainty on the NO_x emission analysis.

[25] Additional constraints from observations of other chemical species could be useful to further improve the model fields and the NO_x emission analysis. An analysis of the background error covariance estimated from the ensemble forecasts (Figure 3a) suggests that observations of chemically related species, such as nitrogen species, terpenes, isoprene, propene, and formaldehyde, with a high sensitivity in the lower troposphere have potential to improve the estimation of NO_x emissions. Most of these observations would also be useful for directly correcting the NO_x concentration in the free troposphere, but with a different order of importance. The correlations also vary significantly with season and height, reflecting changes in the chemical lifetime and meteorological conditions. For instance, the correlation between NO_x emissions and concentrations in the middle troposphere is highest in summer over eastern China (Figure 3b). Highly sensitive NO_x measurements in the middle troposphere (e.g., aircraft observations) and near surface O_3 measurements (though their strong chemical link, Figure 3c) thus have potential to improve estimates of NO_x emissions in summer. Observing system simulation experiments with a careful consideration of the complex chemical interactions, and of vertical sensitivity, error, and sampling of measurements for various species will support future instrumental design to improve the analysis of trace gas concentrations and emissions with the aid of comprehensive chemical data assimilation systems.

[26] **Acknowledgments.** We would like to thank the two anonymous reviewers and the editor for their valuable comments. REAS 2.1 data were provided by Jun-ichi Kurokawa and Toshimasa Ohara. This work was supported by the JSPS Grant-in-Aid for Yong Scientists (B) 24740327.

[27] The Editor thanks two anonymous reviewers for their assistance in evaluating this paper.

References

Boersma, K. F., et al. (2008), Validation of OMI tropospheric NO_2 observations during INTEX-B and application to constrain NO_x emissions over the eastern United States and Mexico, *Atmos. Env.*, *42*, 4480–4497, doi:10.1016/j.atmosenv.2008.02.004.

Eskes, H. J., and K. F. Boersma (2003), Averaging kernels for DOAS total column satellite retrievals, *Atmos. Chem. Phys.*, *3*, 1285–1291, doi:10.5194/acp-3-1285-2003.

Irie, H., K. F. Boersma, Y. Kanaya, H. Takashima, X. Pan, and Z. F. Wang (2012), Quantitative bias estimates for tropospheric NO_2 columns retrieved from SCIAMACHY, OMI, and GOME-2 using a common standard for East Asia, *Atmos. Meas. Tech.*, *5*, 2403–2411, doi:10.5194/amt-5-2403-2012.

Jaeglé, L., L. Steinberger, R. V. Martin, and K. Chance (2005), Global partitioning of NO_x sources using satellite observations: Relative roles of fossil fuel combustion, biomass burning and soil emissions, *Faraday Discuss.*, *130*, 407–423, doi:10.1039/b502128f.

Kurokawa, J., T. Ohara, T. Morikawa, S. Hanayama, J.-M. Greet, T. Fukui, K. Kawashima, and H. Akimoto (2013), Emissions of air pollutants and greenhouse gases over Asian regions during 2000–2008: Regional emission inventory in Asia (REAS) version 2, *Atmos. Chem. Phys. Discuss.*, *13*, 10,049–10,123, doi:10.5194/acpd-13-10049-2013.

Lin, J.-T., Z. Liu, Q. Zhang, H. Liu, J. Mao, and G. Zhuang (2012), Modeling uncertainties for tropospheric nitrogen dioxide columns affecting satellite-based inverse modeling of nitrogen oxides emissions, *Atmos. Chem. Phys.*, *12*, 12,255–12,275, doi:10.5194/acp-12-12255-2012.

Martin, R., D. Jacob, K. Chance, T. Kurosu, P. Palmer, and M. Evans (2003), Global inventory of nitrogen oxide emissions constrained by space-based observations of NO_2 columns, *J. Geophys. Res.*, *108*(D17), 4537, doi:10.1029/2003JD003453.

Miyazaki, K., H. J. Eskes, and K. Sudo (2012a), Global NO_x emission estimates derived from an assimilation of OMI tropospheric NO_2 columns, *Atmos. Chem. Phys.*, *12*, 2263–2288, doi:10.5194/acp-12-2263-2012.

Miyazaki, K., H. J. Eskes, K. Sudo, M. Takigawa, M. van Weele, and K. F. Boersma (2012b), Simultaneous assimilation of satellite NO_2, O_3, CO, and HNO_3 data for the analysis of tropospheric chemical composition and emissions, *Atmos. Chem. Phys.*, *12*, 9545–9579, doi:10.5194/acp-12-9545-2012.

Stavrakou, T., J.-F. Müller, K. F. Boersma, R. J. van der A, J. Kurokawa, T. Ohara, and Q. Zhang (2013), Key chemical NO_x sink uncertainties and how they influence top-down emissions of nitrogen oxides, *Atmos. Chem. Phys. Discuss.*, *13*, 7871–7929, doi:10.5194/acpd-13-7871-2013.

Wang, Y., M. B. McElroy, R. V. Martin, D. G. Streets, Q. Zhang, and T.-M. Fu (2007), Seasonal variability of NO_x emissions over east China constrained by satellite observations: Implications for combustion and microbial sources, *J. Geophys. Res.*, *112*, D06301, doi:10.1029/2006JD007538.

Worden, J., et al. (2009), Observed vertical distribution of tropospheric ozone during the Asian summertime monsoon, *J. Geophys. Res.*, *114*, D13304, doi:10.1029/2008JD010560.

Zhao, C., and Y. Wang (2009), Assimilated inversion of NO_x emissions over east Asia using OMI NO_2 column measurements, *Geophys. Res. Lett.*, *36*, L06805, doi:10.1029/2008GL037123.

Zhao, Y., C. P. Nielsen, Y. Lei, M. B. McElroy, and J. Hao (2011), Quantifying the uncertainties of a bottom-up emission inventory of anthropogenic atmospheric pollutants in China, *Atmos. Chem. Phys.*, *11*, 2295–2308, doi:10.5194/acp-11-2295-2011.